Integrated Schedule and Trajectory Optimization for Connected Automated Vehicles in a Conflict Zone

Zhihong Yao, Haoran Jiang, Yang Cheng, *Member, IEEE*, Yangsheng Jiang, and Bin Ran

***Abstract*— The large-scale application of connected automated vehicles (CAVs) provides new opportunities and challenges for the optimization and management of traffic conflict zones. To improve the traffic efficiency of conflict zones and reduce the travel delay and fuel consumption of CAVs, this paper presents a two-level optimization method of scheduling and trajectory planning for CAVs. At the first level, a 0-1 mixed-integer linear program (MILP) is proposed for vehicles entering scheduling. At the second level, a multi-vehicle optimal trajectory control model is developed based on the optimal vehicle schedule from the first level. Then, to reduce the complexity of solving the multi-vehicle optimal trajectory control model, we transform this model into non-linear programming (NLP) based on the infinitesimal method. Moreover, a rolling optimization strategy is developed to facilitate field application. Numerical simulation experiments of different traffic scenarios are conducted, and the results show that the proposed method can effectively reduce vehicle delays and fuel consumption, compared with the first-in-first-out (FIFO) method. The numerical results show that the vehicle delay can be reduced by up to 54% and fuel consumption by up to 34% under different traffic demands. Sensitivity analysis indicates that the performance of the proposed method is mainly determined by the minimum safety time interval of vehicles entering the conflict zone.**

***Index Terms*— Connected automated vehicles, optimal scheduling, MILP, conflict zone, trajectories planning.**

I. Introduction

TRAFFIC conflict zones [1]–[4] (e.g. ramps, intersections, work-zones) generally refer to areas of elevated collision risks for vehicles. Studies show that conflict zones not only have potential safety hazards but also are the primary nodes causing vehicle delays and fuel consumption [3], [4]. Therefore, most existing research [5]–[11] is to alleviate collision through scheduling, which is controlling the time of vehicles passing through the conflict zones. However, most of these methods are only for human-driven vehicles (HDVs), and cannot directly optimize and control the HDVs. In recent years, the development of connected automated vehicles (CAVs) technologies [12]–[14], have enabled the information exchange among vehicles (V2V) and between vehicles and infrastructure (V2I) through wireless communication by installing onboard units (OBUs) and roadside units (RSUs). Moreover, the latest research [15] shows that by 2045, the penetration rate of CAVs on the road would reach a high level, which can reach 87.2% if conditions permit. Therefore, the large-scale application of CAVs presents new opportunities and challenges for the operation, management, and optimization of the conflict zones [16]–[21].

Many scholars have studied the application of CAVs in transportation. These studies mainly focus on traffic flow characteristics [22]–[24], vehicle trajectory optimization [25]–[28], and traffic signal control optimization [9], [29], [30]. In this study, we focus on the optimization of scheduling and trajectory of CAVs. He *et al.* [25] proposed an optimal speed model to provide speed guidance for CAVs considering the influence of vehicle queues at intersections. The case study showed that speed guidance could reduce vehicles' travel time and fuel consumption by 9% and 29%, respectively. However, this study did not consider the interaction between vehicles. Wan *et al.* [31] constructed a vehicle speed guidance model with an analytical solution for the mixed traffic flow for a fixed signal timing plan. The simulation result showed that the fuel consumption of the mixed platoon could be greatly reduced with the increase of the penetration rate of CAVs. Zhao *et al.* [32] proposed a predictive control model of speed guidance for the mixed platoon consisting of CAVs and HDVs. The simulation results showed that the proposed model could effectively smooth the vehicle trajectory and reduce fuel consumption. These studies provide speed guidance for a fixed signal timing plan only, not considering optimizing traffic signal timing. Therefore, some scholars studied coordinated optimization of traffic signals and vehicle trajectories. Yu *et al.* [8] investigated a traffic signal and vehicle trajectory optimization model based on mixed-integer programming at an isolated intersection. Simulation results validated the advantages of the proposed control method over vehicle-actuated control in terms of intersection capacity, vehicle delays, and CO_2 emissions. Feng *et al.* [33] proposed a two-stage optimization model for traffic signal and vehicle trajectory control, in which dynamic programming algorithms and optimal control theories were used to obtain

Manuscript received February 19, 2020; revised June 28, 2020 and August 16, 2020; accepted September 25, 2020. Date of publication October 13, 2020; date of current version March 9, 2022. This work was supported in part by the Chinese National Natural Science Fund under Grant 52002339, Grant 71901183, and Grant 71771190, in part by the Innovation Center Project of Chengdu Jiao Da Big Data Technology Co., Ltd. under Grant JDSKCXZX202003, and in part by the Open Fund Project of Chongqing Key Laboratory of Traffic and Transportation under Grant 2018TE01. The Associate Editor for this article was I. Papamichail. *(Corresponding author: Zhihong Yao.)*

Zhihong Yao is with the National Engineering Laboratory of Integrated Transportation Big Data Application Technology, National United Engineering Laboratory of Integrated and Intelligent Transportation, School of Transportation and Logistics, Institute of System Science and Engineering, Southwest Jiaotong University, Sichuan 610031, China (e-mail: zhyao@swjtu.edu.cn).

Haoran Jiang and Yangsheng Jiang are with the National Engineering Laboratory of Integrated Transportation Big Data Application Technology, School of Transportation and Logistics, Southwest Jiaotong University, Sichuan 610031, China (e-mail: 1072135297@qq.com; jiangyangsheng@swjtu.cn).

Yang Cheng and Bin Ran are with the Department of Civil and Environmental Engineering, University of Wisconsin–Madison, Madison, WI 53706 USA (e-mail: cheng8@wisc.edu; bran@wisc.edu).

Digital Object Identifier 10.1109/TITS.2020.3027731

the signal timing plan and vehicle trajectory of the intersection, respectively. The simulation showed that compared with fixed traffic signal timing and adaptive control, the proposed model could reduce vehicle's delays and fuel consumption simultaneously. However, the basic assumption of these studies is to use traffic signals to control vehicles, while coordination and schedule optimization between vehicles are not considered.

With the large-scale application of CAVs, the vehicle would be able to independently and cooperatively pass through the conflict zones without a traffic signal [34]. The basic idea is that the conflict zones do not need signal control, and the time when the vehicle enters the conflict zone is controlled and optimized to avoid the collision. Tachet *et al.* [35] developed a slot-based intersection control method, which is similar to slot-based systems used in aerial traffic. The theoretical analysis results showed that compared with the signal control system, the proposed method has the potential to double the capacity and significantly reduce the delay. Li and Wang [36] first conceptually proposed a future intersection management model, in which the intersection has no traffic signals and the vehicle could determine the timing of entering through cooperation and interaction, thereby avoiding collision between vehicles [37]. Fayazi and Vahidi [17], Fayazi *et al.* [38] constructed a mixed-integer linear program model to optimize the timing of vehicles entering intersections. The model used the form of a multi-objective linear combination to achieve the effect of vehicle delay reduction. The result showed that the MILP improved the average travel time per vehicle and the average stopped delay per stopped vehicle by 7.5% and 52.4%, respectively. Dresner and Stone [39] developed an alternative mechanism for coordinating the movement of autonomous vehicles through intersections based on a multiagent system. The experimental results strongly proved the effectiveness of the proposed method. However, the above studies only studied how to control or optimize the time when the vehicle entered the conflict zones and did not consider the optimization of vehicle trajectory. He *et al.* [18] designed a future intersection management control model in CAVs environment. This model avoided collisions between vehicles by controlling the time of the vehicle to enter the intersection and optimizing vehicles' trajectory. The simulation results showed that the model significantly improved the intersection capacity and reduced fuel consumption. However, the basic assumption of this study was that the vehicle enters the intersection based on the first-in-first-out (FIFO) rule. Thus, the vehicle entry sequence was not optimized. To find the optimal sequence and trajectory of vehicles, Rios-Torres and Malikopoulos [40] presented an optimization framework and an analytical closed-form solution to coordinate vehicles at merging zones. The results showed that coordination of vehicles can significantly reduce both fuel consumption and travel time. Wang *et al.* [41] proposed a distributed consensus protocol approach for CAVs to cooperate by V2X communications. The simulation study indicated that the approach benefits traffic throughput and energy saving. However, the approach manages CAV based on relevant rules, and does not use the optimization method to optimize the vehicle timing and trajectory as a whole.

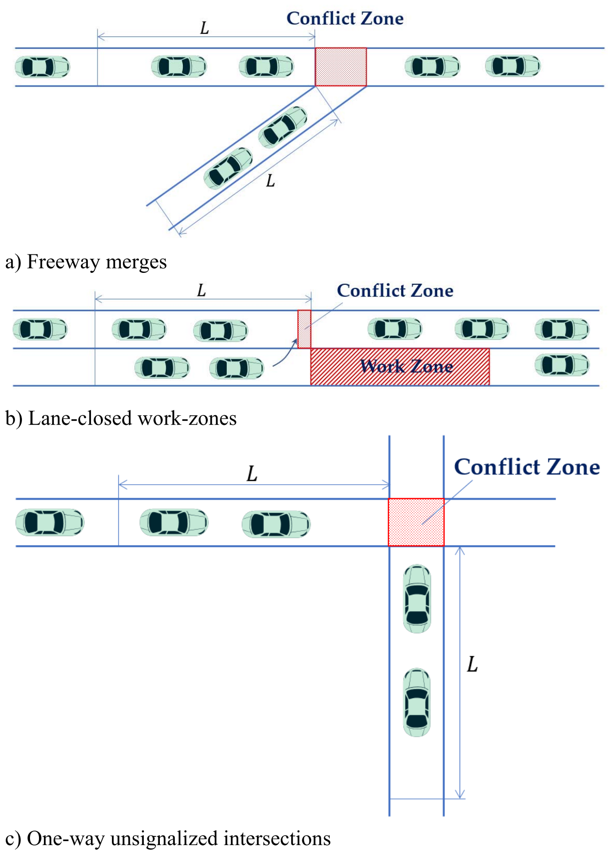

Fig. 1. Common conflict zones.

As far as we know, most of the existing research does not consider optimizing the timing and trajectory of vehicles entering the conflict zones simultaneously. Therefore, to address this gap, this study proposes a two-level model to optimize schedule and trajectories for CAVs in conflict zones.

The remainder of this paper is structured as follows. Section 2 describes the problem of the optimization of the conflict zones of CAVs. A two-level optimization model is proposed in Section 3. Section 4 introduces a rolling optimization strategy. Numerical simulation and discussion are conducted in Section 5. Finally, Section 6 ends this paper with conclusions and future work.

II. Problem Settings

Traffic conflict zones have a common function, which is defined as separating vehicles with conflicting movements into appropriate batches without inter-batch conflicts to let them pass sequentially in a relatively fair manner. As shown in Fig. 1, common conflict zones include freeway merges, lane-closed work-zones, and one-way unsignalized intersections. In particular, we assume that vehicles do not change lanes in the control zone, that is, the multi Lane problem can be described as a one-lane problem, and we only consider the one-lane problem in the Fig. 1c). The vehicle needs to slow down and observe other vehicles from different directions to ensure safety before it enters the conflict zone. This behavior would directly lead to vehicle delays and extra fuel consumption. In a CAV environment, CAVs can pass through the conflict zone with a higher speed based on an optimal arrival schedule. Therefore, vehicle delays would be reduced significantly. Moreover, based on the optimal arrival schedule, the vehicle trajectory is further optimized to reduce fuel consumption. This study aims to optimize both schedule and trajectories for CAVs in a conflict zone. Therefore, the proposed method can not only avoid vehicle collisions but also reduce vehicle delays and fuel consumption.

Fig. 1 shows that the conflict zones studied in this paper generally consist of two conflicting directions, each of which is represented by i, where $i \in \mathfrak{I} = \{1, 2\}$. The length of the control zone is L, the free-flow speed of the road segment in each direction is $v_i^f, i \in \mathfrak{I}$. Given the optimization interval ΔT, if the current time is T_0, the optimized time interval is $[T_0, T_0 + \Delta T]$. During this time interval, the set of vehicles entering the control zone in the direction i is $\mathcal{N}_i$. Therefore, all vehicles entering the control zone during the time interval are represented as $j \in \mathcal{N}_i = \{1, 2, \cdots, N_i\}, i \in I$. Assume that t_{ij}^- represents the time when the jth vehicle enters the control zone of the ith direction. t_{ij}^* and t_{ij}^+ are the ideal time and the actual time when the jth vehicle enters the conflict zone of the ith direction, respectively. The problem in this study is expressed as a two-level optimization problem: (1) the first level is to optimize the time t_{ij}^+ of all CAVs arriving at the conflict zone for achieving the minimum delay; (2) in the second level, based on the optimal arrival time t_{ij}^+ in the first level, the safety distance between the vehicles in the same direction, the start and end states (time, position and speed, etc.) constraints are considered to optimize vehicle trajectories for minimizing fuel consumption. The following section would discuss in detail how to propose the two-level optimization model.

III. Two-Level Optimization Model

A. Assumptions and Limitations

To facilitate the development of our model, there are some necessary assumptions and limitations.

(1) CAVs are in regular operation without considering its failure, and all CAVs can be controlled and optimized by infrastructure.

(2) Control and communication delay of CAVs are not considered in this study.

(3) To reduce vehicle delay, refer to Zhao *et al.* [32], all CAVs pass the downstream intersection by the desired speed.

(4) In the control zone, vehicles are not allowed to change lanes. Therefore, this study does not consider lane-changing behavior in the control zone, which can be referred to Yu *et al.* [8].

B. Scheduling Optimization Model

A one-way unsignalized intersections from Fig. 1c) is an example. The east-west direction of the main road is set to $i = 1$, and the north-south direction of the secondary road is set to $i = 2$. A simple example is used to illustrate the solution space for vehicles' schedule optimization. We assume that there are two vehicles on the main road and secondary road to pass through the conflict zone in the optimized time interval. The vehicles of the main road are labeled 1 and 2, while the vehicles in the secondary road are labeled 3 and 4. Meanwhile, vehicles in the same direction follow the first-in-first-out (FIFO) rule, which means the vehicles entering the conflict zone in the same direction are unchanged (i.e., Vehicle 1 arrives and passes the conflict zone before Vehicle 2). Therefore, the timing schedule optimization problem is to optimize the timing of vehicles entering the conflict zone for minimizing the average delay. The following is a brief analysis of the timing schedule of the main road and the ramp with only two vehicles, as shown in Table I.

TABLE I
Timing Schedule Analysis

Index	Schedule
1	1→2→3→4
2	1→3→2→4
3	1→3→4→2
4	3→4→1→2
5	3→1→4→2
6	3→1→2→4

Table I indicates that when there are two vehicles on the main road and the secondary road, there are six kinds of timing schedules for passing through the conflict zone. Furthermore, if there are m vehicles on the main road and n vehicles on the secondary road. According to the theory of arrangement and combination, we can know that the number of possible timing sequences is $A_{m+n}^{m+n} \big/ \left(A_m^m \times A_n^n\right)$. Therefore, as the number of vehicles increases, the number of timing sequences may be huge. The enumeration method would not be applicable to solve this problem. The following section would specifically propose a mixed-integer linear program (MILP) model to optimize the schedule of vehicles passing through the conflict zones.

1) Time Parameter Analysis: The timing schedule optimization model contains many time parameters, such as the time vehicles enter the control zone, the ideal time, and the actual time for vehicles to reach the conflict zone. In a CAV environment, we assume that the time (t_{ij}^-) when vehicles enter the control zone can be estimated accurately [42]. Therefore, this study assumes that the time when the vehicle enters the control zone in the future time interval ΔT is known and defined as $t_{ij}^-, \forall i \in \mathfrak{I}, j \in \mathcal{N}_i$. Then, the ideal time for vehicles to reach the conflict zone can be estimated based on the distance from the boundaries of the control zone to the conflict zone and the free-flow speed of the road segment.

$$t_{ij}^* = t_{ij}^- + \frac{L}{V_i}, \quad \forall i \in \mathfrak{I}, \quad j \in \mathcal{N}_i. \tag{1}$$

where t_{ij}^- is the time for the jth vehicles of the ith direction enters the control zone; t_{ij}^* is the ideal time for the jth vehicles of the ith the direction enters the conflict zone; V_i is the free-flow speed in the ith direction; L is the distance from the boundaries of the control zone to the conflict zone, a common assumption is that the coverage of the communication is a spherical region, so the distance in each direction is equal [43], [44].

2) Objective Function: After relevant time parameters are determined, the objective function for vehicle delay is obtained. The delay of vehicles is defined as the actual travel time minus the ideal travel time (travel with free-flow speed). Therefore, the total delay of vehicles in the ith direction is formulated as

$$\mathcal{D}_i = \sum_{j \in \mathcal{N}_i} \left(t_{ij}^{+} - t_{ij}^{-} - \frac{L}{V_i} \right), \quad \forall i \in \mathcal{I}. \tag{2}$$

where $\mathcal{D}_i$ is the total delay of vehicles in the ith direction; t_{ij}^{+} is the actual time when the jth vehicle in the ith direction reaches the conflict zone, which is a variable that needs to be optimized.

The average delay of all vehicles in the optimization time interval is calculated based on Eq. (2), as shown in Eq. (3).

$$d = \frac{1}{\sum\limits_{i \in \mathcal{I}} N_i} \sum_{i \in \mathcal{I}} \sum_{j \in \mathcal{N}_i} \left(t_{ij}^{+} - t_{ij}^{-} - \frac{L}{V_i} \right) \tag{3}$$

where d is the average delay of all vehicles within the optimization time interval; N_i is the number of vehicles in the ith direction during the optimization time interval, $N_i = |\mathcal{N}_i|$.

3) Constrains: The actual time of vehicles to reach the conflict zone is not less than the ideal time, so this constraint can be written in Eq. (4).

$$t_{ij}^{+} \geq t_{ij}^{*}, \quad \forall i \in \mathcal{I}, j \in \mathcal{N}_i. \tag{4}$$

In this study, we only consider a single lane, so there is no lane change behavior. Therefore, the first-in-first-out (FIFO) rule is adopted for vehicles in the same direction. To ensure that two adjacent vehicles in the same direction pass through the conflict zone safely, the time interval between them must not be less than τ. This constraint is expressed in Eq. (5).

$$t_{ij}^{+} \geq t_{i(j-1)}^{+} + \tau, \quad \forall i \in \mathcal{I}, j \in \mathcal{N}_i. \tag{5}$$

where τ is the minimum time interval between two adjacent vehicles in the same direction to pass through the conflict zone.

Furthermore, a specific time interval should be ensured for two adjacent vehicles in different directions to pass through the conflict zone. We assume that the minimum time interval between two adjacent vehicles in different directions passing through the conflict zone is ω. To facilitate our model development, we use the time interval of any two vehicles passing through the conflict zone in different directions to formulate this constraint, as shown in Eq. (6).

$$\left| t_{1,m}^{+} - t_{2,n}^{+} \right| \geq \omega, m \in \mathcal{N}_1, n \in \mathcal{N}_2. \tag{6}$$

where ω is the minimum time interval between two adjacent vehicles in different directions to pass through the conflict zone.

The absolute value in Eq. (6) makes the optimization problems nonlinear, which is not easy to solve. To transform nonlinear constraints into linear constraints, a 0-1 variable $B_{m,n}$ is introduced. Therefore, Eq. (6) is rewritten as follows:

$$\begin{cases} t_{1,m}^{+} - t_{2,n}^{+} \geq \omega, & \text{if } B_{m,n} = 1 \\ t_{2,n}^{+} - t_{1,m}^{+} \geq \omega, & \text{if } B_{m,n} = 0, \end{cases} \quad m \in \mathcal{N}_1, n \in \mathcal{N}_2. \tag{7}$$

where $B_{m,n}$ is a 0-1 variable, $B_{m,n} = 1$ indicates that the vehicle numbered n in direction 1 passes the conflict zone first compared with the vehicle numbered m in direction 2; otherwise $B_{m,n} = 0$.

Further, Eq. (7) is converted into the following two equivalent constraint formulas based on a larger value M.

$$B_{m,n} \times M + t_{2,n}^{+} - t_{1,m}^{+} \geq \omega, \quad m \in \mathcal{N}_1, n \in \mathcal{N}_2. \tag{8}$$

$$\left(1 - B_{m,n}\right) \times M + t_{1,m}^{+} - t_{2,n}^{+} \geq \omega, \quad m \in \mathcal{N}_1, n \in \mathcal{N}_2. \tag{9}$$

4) Solution Algorithm: From the above analysis, the objective function Eq. (3) and the constraints Eqs. (4-9) of the proposed model are linear. Thus, the proposed optimization model is linear programming (LP), which is directly solved by commercial software, such as MATLAB, CPLEX, and Lingo. However, the value of M has a significant influence on the efficiency of the solving algorithm. To improve the calculation efficiency of the algorithm, we assume that the actual travel time of the vehicle is not more than θ times the free-flow travel time, where θ is greater than 1. To sum up, Eq. (4) can be specified as

$$t_{ij}^{-} + \frac{\theta L}{V_i} \geq t_{ij}^{+} \geq t_{ij}^{-} + \frac{L}{V_i}, \quad \forall i \in \mathcal{I}, j \in \mathcal{N}_i. \tag{10}$$

Besides, the value of M only needs to be higher than the maximum possible time, which equals to the vehicle to reach the conflict zone within the optimized time interval minus the minimum possible time. Therefore, M is defined as follows

$$\begin{aligned} M = \max &\left(t_{1,N_1}^{-} + \frac{\theta L}{V_1}, t_{2,N_2}^{-} + \frac{\theta L}{V_2} \right) \\ &- \min \left(t_{1,1}^{-} + \frac{L}{V_1}, t_{2,1}^{-} + \frac{L}{V_2} \right). \end{aligned} \tag{11}$$

where N_1 and N_2 are the last vehicle entering the control zone in direction 1 and direction 2 within the optimized time interval, respectively.

In summary, the scheduling of the vehicle entering the conflict zone is a linear programming model, as shown in Eq. (12).

$$\begin{aligned} &\min \mathcal{D} = \frac{1}{\sum_{i \in \mathcal{I}} N_i} \sum_{i \in \mathcal{I}} \sum_{j \in \mathcal{N}_i} \left(t_{ij}^{+} - t_{ij}^{-} - \frac{L}{V_i} \right) \\ &s.t. \begin{cases} t_{ij}^{-} + \dfrac{\theta L}{V_i} \geq t_{ij}^{+} \geq t_{ij}^{-} + \dfrac{L}{V_i}, \forall i \in \mathcal{I}, j \in \mathcal{N}_i. \\ t_{ij}^{+} \geq t_{i(j-1)}^{+} + \tau, \forall i \in \mathcal{I}, j \in \mathcal{N}_i. \\ B_{m,n} \times M + t_{2,n}^{+} - t_{1,m}^{+} \geq \omega, m \in \mathcal{N}_1, n \in \mathcal{N}_2. \\ (1 - B_{m,n}) \times M + t_{1,m}^{+} - t_{2,n}^{+} \geq \omega, m \in \mathcal{N}_1, n \in \mathcal{N}_2. \\ B_{m,n} \text{ is a } 0, 1 \text{ variable} \end{cases} \end{aligned} \tag{12}$$

When the flow rate is low, the vehicle can pass through the conflict zone without delay, so the value of θ is very close to 1 in this case; otherwise, the value of θ should be

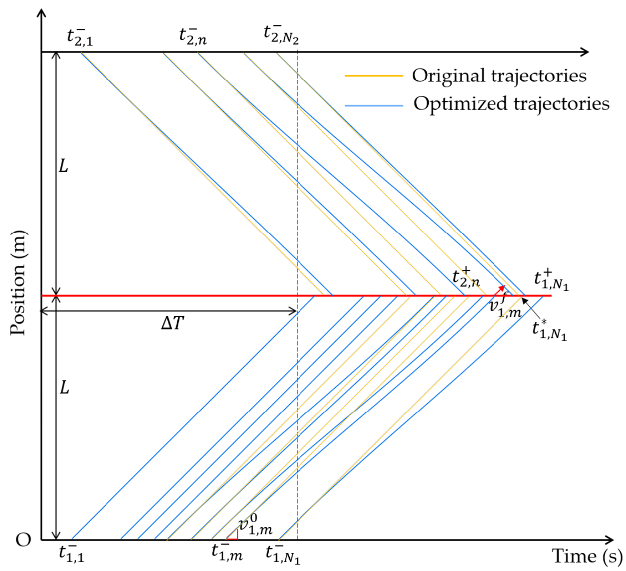

Fig. 2. Schematic diagram of trajectory optimization.

more significant. To ensure the efficiency of the algorithm, we set reasonable θ under different flow conditions.

C. Trajectory Optimization Model

1) Problem Analysis: Based on the optimal schedule, the space-time diagram of the optimal trajectory is shown in Fig. 2. In the trajectory optimization model, the optimized trajectory minimizes the fuel consumption of all vehicles during the optimized time interval based on the initial and end state of vehicles. Besides, the minimum safety interval between vehicles in the same direction must be considered. Therefore, the trajectory optimization is an optimal control problem [25], [31], [32], [45], [46].

2) Objective Function: Based on existing research [46]–[50], the fuel consumption of vehicles is related to its speed and acceleration. The instantaneous gasoline consumption function proposed by Akcelik [47] is adopted in this study. The gasoline consumption rate is formulated according to the instantaneous velocity and acceleration of a vehicle.

$$F(v, a; t) = \begin{cases} \alpha + \beta_1 \ P(t) + \left[\dfrac{\beta_2 \ ma(t)^2 v(t)}{1000}\right]_{a>0}, & P(t)P > 0 \\ \alpha, & P(t) \leq 0. \end{cases} \tag{13}$$

where F is the instantaneous fuel consumption of vehicles at the time t; α is the fuel consumption rate at the time of vehicle idling; m is the mass of the vehicle; β_1 is an efficiency parameter which relates fuel consumed to the energy provided by the engine; β_2 is an efficiency parameter, which relates fuel consumed during positive acceleration to the product of inertia energy and acceleration; $v(t)$ and $a(t)$ represent speed and acceleration of vehicle at the time t, respectively; $P(t)$ is the total power of vehicles, which is expressed by Eq. (14).

$$P(t) = d_1 v(t) + d_2 v(t)^2 + d_3 v(t)^3 + \frac{ma(t)v(t)}{1000}. \tag{14}$$

where d_1, d_2 and d_3 are represent rolling, engine and aerodynamic drag, respectively.

Based on the literature [47], the values of the relevant parameters in Eqs. (13) and (14) are: $\alpha = 0.666$mL/s, $\beta_1 = 0.072$ ml/kJ, $\beta_2 = 0.0344$mL/(kJ(m/s)^2), $d_1 = 0.269$kN, $d_2 = 0.0171$kN/(m/s), $d_3 = 0.000672$ kN/(m/s)^2, $m = 1680$ kg.

To sum up, the total fuel consumption G_i of the vehicle in the ith conflict direction during an optimized time interval is shown as

$$\mathcal{G}_i = \sum_{j \in \mathcal{N}_i} \int_{t_{ij}^-}^{t_{ij}+} F\left(\dot{x}_{ij}(t), \ddot{x}_{ij}(t); t\right) dt, \quad \forall i \in \mathcal{I}. \tag{15}$$

where $\dot{x}_{ij}(t)$ and $\ddot{x}_{ij}(t)$ are the speed and acceleration of the jth vehicle in the ith direction at the time t, respectively.

The average fuel consumption of all vehicles is obtained, as shown in Eq. (16).

$$g = \frac{1}{\sum_{i \in \mathcal{I}} N_i} \sum_{i \in \mathcal{I}} \sum_{j \in \mathcal{N}_i} \int_{t_{ij}^-}^{t_{ij}^+} F\left(\dot{x}_{ij}(t), \ddot{x}_{ij}(t); t\right) dt. \tag{16}$$

where g is the average fuel consumption of all vehicles during the optimized time interval.

3) Constraints: The vehicle should satisfy the following dynamic equations at any time.

$$\dot{x}_{ij}(t) = \frac{dx_{ij}(t)}{dt}, \quad \forall t \in \left[t_{ij}^-, t_{ij}^+\right], i \in \mathcal{I}, j \in \mathcal{N}_i. \tag{17}$$

$$\ddot{x}_{ij}(t) = \frac{d\dot{x}_{ij}(t)}{dt}, \quad \forall t \in \left[t_{ij}^-, t_{ij}^+\right], i \in \mathcal{I}, j \in \mathcal{N}_i. \tag{18}$$

The vehicle's initial and the termination state satisfy the following constraints

$$x_{ij}\left(t_{ij}^-\right) = 0, \dot{x}_{ij}\left(t_{ij}^-\right) = v_{ij}^0, \ddot{x}_{ij}\left(t_{ij}^-\right) = 0, \quad \forall i \in \mathcal{I}, j \in \mathcal{N}_i. \tag{19}$$

$$x_{ij}\left(t_{ij}^+\right) = L, \dot{x}_{ij}\left(t_{ij}^+\right) = v_{ij}^f, \ddot{x}_{ij}\left(t_{ij}^+\right) = 0, \quad \forall i \in \mathcal{I}, j \in \mathcal{N}_i. \tag{20}$$

Meanwhile, to ensure the safety of the vehicle, the minimum safety spacing requirements must be met between the adjacent vehicles in the same direction (segment), which is written as follows:

$$x_{i(j-1)}(t) - x_{ij}(t) \geq s_0 + l, \quad \forall i \in \mathcal{I}, j \in \mathcal{N}_i \setminus \{1\}, t_{ij} \in \left[t_{i(j-1)}^-, t_{ij}^+\right]. \tag{21}$$

where s_0 is the minimum safe spacing between adjacent vehicles, l is the length of vehicle, which is generally set at 5 m.

Besides, the speed and acceleration of the vehicle must meet the relevant constraints during driving, which is formulated as follows.

$$0 \leq \dot{x}_{ij}(t) \leq v_{\max}, \quad \forall t \in \left[t_{ij}^-, t_{ij}^+\right], i \in \mathcal{I}, j \in \mathcal{N}_i. \tag{22}$$

$$a_{\min} \leq \ddot{x}_{ij}(t) \leq a_{\max}, \quad \forall t \in \left[t_{ij}^-, t_{ij}^+\right], i \in \mathcal{I}, j \in \mathcal{N}_i. \tag{23}$$

where $a_{\min}$ and $a_{\max}$ are the minimum and maximum acceleration of the vehicle, respectively.

4) Solution Algorithm: Based on the above analysis, the vehicle trajectory optimization model is an optimal control model. We transform it into nonlinear programming (NLP) to solve. Therefore, the infinitesimal method can be used to process the optimal control model discretely.

We assume δ is a sufficiently small number, so $t_{ij}^{-} \leq k\delta \leq t_{ij}^{+}, k_{ij}^{-}\delta = t_{ij}^{-}, k_{ij}^{+}\delta = t_{ij}^{+}$. The objective function Eq. (16) is defined as follows.

$$g = \frac{1}{\sum\limits_{i \in \mathcal{I}} N_i} \sum_{i \in \mathcal{I}} \sum_{j \in \mathcal{N}_i} \sum_{k \in \left[k_{ij}^{-}, k_{ij}^{+}\right]} F\left(\dot{x}_{ij}[k], \ddot{x}_{ij}[k]; t\right)\delta \tag{24}$$

Similarly, the constraints of dynamic equations are formulated as follows.

$$\dot{x}_{ij}[k] = \frac{x_{ij}[k] - x_{ij}[k-1]}{\delta}, \quad \forall k \in \left[k_{ij}^{-}+1, k_{ij}^{+}\right], i \in \mathcal{I}, j \in \mathcal{N}_i. \tag{25}$$

$$\ddot{x}_{ij}[k] = \frac{\dot{x}_{ij}[k+1] - \dot{x}_{ij}[k]}{\delta} = \frac{x_{ij}[k+1] - 2x_{ij}[k] + x_{ij}[k-1]}{\delta^2}, \quad \forall k \in \left[k_{ij}^{-}+1, k_{ij}^{+}-1\right], i \in \mathcal{I}, j \in \mathcal{N}_i. \tag{26}$$

The initial and termination state constraints are

$$x_{ij}\left[k_{ij}^{-}\right] = 0, \dot{x}_{ij}\left[k_{ij}^{-}\right] = v_{ij}^{0}, \ddot{x}_{ij}\left[k_{ij}^{-}\right] = 0, \quad \forall i \in \mathcal{I}, j \in \mathcal{N}_i. \tag{27}$$

$$x_{ij}\left[k_{ij}^{+}\right] = L, \dot{x}_{ij}\left[k_{ij}^{+}\right] = v_{ij}^{f}, \ddot{x}_{ij}\left[k_{ij}^{+}\right] = 0, \quad \forall i \in \mathcal{I}, j \in \mathcal{N}_i. \tag{28}$$

The positional constraints of adjacent vehicles can be expressed as follows.

$$x_{i(j-1)}[k] - x_{ij}[k] \geq s_0, \quad \forall i \in \mathcal{I}, n \in \mathcal{N}_i \setminus \{1\}, t_{ij} \in \left[k_{i(j-1)}^{-}, k_{ij}^{+}\right]. \tag{29}$$

The speed and acceleration constraints of the vehicle can be written as follows.

$$0 \leq \dot{x}_{ij}[k] \leq v_{\max}, \quad \forall k \in \left[k_{ij}^{-}, k_{ij}^{+}\right], i \in \mathcal{I}, j \in \mathcal{N}_i. \tag{30}$$

$$a_{\min} \leq \ddot{x}_{ij}[k] \leq a_{\max}, \quad \forall k \in \left[k_{ij}^{-}, k_{ij}^{+}\right], i \in \mathcal{I}, j \in \mathcal{N}_i. \tag{31}$$

Above all, the objective function of the model is nonlinear, as shown in Eq. (24); the constraint conditions are Eqs. (25)-(31), all of which are linear formulas. Therefore, this model is nonlinear programming (NLP), which can be solved by IPOPT or MATLAB.

IV. Rolling Optimization Strategy

In the actual optimization, a rolling optimization strategy can be adopted [51]. There are two main reasons for consideration. Firstly, we assume that the time that vehicles reach the control boundary can be calculated accurately in the CAVs environment [42]; but the longer the prediction time interval, the more difficult the prediction is. Therefore, short-term (such as 10 seconds) predictions are easier to implement. Secondly, when the optimization time interval (ΔT) is higher than a specific value, the vehicles in different optimization time intervals would not affect the optimal sequence. Therefore, the sequence of vehicles in different optimization time intervals can be optimized independently. To sum up, we assume that the schedule and trajectories of CAVs passing through the conflict zone are optimized every ΔT time interval, and the total optimization duration is T. The specific rolling optimization strategy is as follows.

Step 1. Initializing parameter: θ, and $t = 0$;

Step 2. Calculate the current optimization time interval $[t, t + \Delta T]$;

Step 3. Predict the time of CAVs arriving in the control zone within the current optimization time interval, $t_{ij}^{-}, \forall i \in \mathcal{I}, j \in \mathcal{N}_i$;

Step 4. The first-level of linear programming model in Eq. (12) is adopted to optimize the optimal schedule of CAVs passing through the conflict zone: $t_{ij}^{+}, \forall i \in \mathcal{I}, j \in \mathcal{N}_i$ and vehicle delay $\mathcal{D}$;

Step 5. Based on the optimal scheduling $t_{ij}^{+}, \forall i \in \mathcal{I}, j \in \mathcal{N}_i$ calculated by **Step 4**, the second-level nonlinear optimization model is adopted to solve the optimal vehicle trajectories and fuel consumption: $x_{ij}, \forall i \in \mathcal{I}, j \in \mathcal{N}_i$ and $\mathcal{G}$;

Step 6. Let $t = t + \Delta T$. If $t > T$, the optimization ends, output the optimal schedule and trajectories, the vehicle delay and fuel consumption; otherwise, go to **Step 2**.

To ensure the safety distance of any adjacent vehicle, the last vehicle in the previous optimization time interval and the first vehicle in the current optimization time interval should satisfy the minimum safety head time constraint. If it is not satisfied, the time sequence needs to be time-shifted, as shown in Eqs. (32) and (33).

$$t_{ij}^{+} = \begin{cases} t_{ij}^{+'}, \\ \quad \text{if } t_{i1}^{+'} \geq T_p + \xi \\ t_{ij}^{+'} + (T_p + \xi - t_{i1}^{+'}), \\ \quad \text{if } t_{i1}^{+} < T_p + \xi, \end{cases} \quad \forall i, p \in \mathcal{I}, j \in \mathcal{N}_i. \tag{32}$$

$$\xi = \begin{cases} \tau, & \text{if } i = p \\ \omega, & \text{if } i \neq p \end{cases} \tag{33}$$

where $t_{ij}^{+'}$ is the optimal timing without considering the rolling optimization strategy; T_p represents the time of the last vehicle from direction p passing through the conflict zone during the previous optimized time interval; ξ indicates the minimum safe time headway. If the first vehicle within the next optimized time interval belongs to the same direction as the last vehicle within the previous optimized time interval, then $\xi = \tau$; otherwise, $\xi = \omega$.

Based on the rolling optimization strategy, the algorithm can find the optimal solution in 1 second on a general laptop computer. Besides, with the rise of computational power and edge computing, the efficiency of the algorithm would be further improved. Therefore, the algorithm can be used in practical applications.

TABLE II

SIMULATION PARAMETER SETTINGS

Variables	Value	Unit
T	900	s
ΔT	10	s
L	300	m
V_i	15	m/s
τ	1.0	s
ω	1.5	s
θ	2	-
v_{ij}^0	15	m/s
v_{ij}^f	15	m/s
$v_{\min}$	0	m/s
$v_{\max}$	15	m/s
$a_{\min}$	-6	m/s^2
$a_{\max}$	3	m/s^2
s_0	5	m
δ	0.1	s

TABLE III

DIFFERENT TRAFFIC DEMANDS

Number	Flow (veh/h)	
	Direction 1	Direction 2
1	900	900
2	1,200	900
3	1,200	1,200
4	1,800	1,200
5	1,800	1,800
6	2,400	1,800

V. NUMERICAL SIMULATION AND ANALYSIS

A. Simulation Parameter Settings

Referring to the literature [8], [33], we assume that vehicle arrivals follow a Poisson process, the total simulation time is 900 s, and the optimization interval is 10 s. Based on the Dedicated Short-Range Communication (DSRC) technique [43], [44], the control area length is set to 300 m. Take one-way unsignalized intersections in Fig. 1c) as an example, the parameters are shown in Table II. In particular, the simulation experiment is a numerical simulation. Therefore, pre-warm time is not included in the duration of T, which only contains optimization and data collection time. Moreover, for other conflict zones in Fig.1, different parameters (e.g., desired speed, desired gap, location constraints) need to be set according to the actual situation. Besides, we assume that all CAVs can be controlled in the simulation experiment, regardless of the actual vehicle uncontrolled or communication failure and other abnormal factors.

To verify the performance of the proposed model and algorithm, the proposed method is tested in different traffic demands (Table III) and compared with the FIFO-based method [41]. Specifically, different simulation traffic scenarios are shown in Table IV.

All simulation scenarios are implemented by the MATLAB platform in the computer with CPU i7-6500U and 8GB the memory. Meanwhile, each set of simulation scenarios is simulated 10 times with different random seeds to capture the influence of randomness. Therefore, combined with the rolling optimization strategy in Section IV, the detailed pseudocode of the simulation experiment is presented in the Appendix. Based on the simulation, the results are shown in Table IV and Table V.

As seen from Table IV, the optimized vehicle delays in the six scenarios are less than the delays obtained from implementing the FIFO-based method. Moreover, the percentage of delay reduction for all six scenarios is above 10%, and the maximum vehicle delay can be reduced by 54.23%. Besides, Fig. 3 shows the space-time trajectory of CAVs. There is no intersection trajectory in Fig. 3, which verifies the correctness of the optimization results of the proposed method. Moreover, as shown in the A areas in Fig. 3, when the schedule of vehicles is not optimized, vehicles from different conflict directions cross the conflict zone (A areas in Fig. 3). This means ω will appear more frequently. However, the proposed method can optimize the schedule of vehicles and avoid the occurrence of ω and increase the occurrence of τ (B areas in Fig. 3). Moreover, because ω is larger than τ, vehicle delay of the proposed method is smaller than the FIFO-based method.

Table V presents the proposed method effectively reduces fuel consumption compared with the FIFO-based method. With the increase of flow rate, the reduction of fuel consumption is more significant, and the fuel consumption can reduce by up to 34.36%. The result illustrates that although vehicle trajectories optimized by the same method, the fuel consumption of the proposed method is smaller. In other words, the vehicle trajectories in the space-time figure are shorter, and the time interval in which the vehicle accelerates and decelerates during driving is shorter. From the existing research [8], [33], the fuel consumption of vehicles is related to the magnitude and duration of the acceleration and deceleration of vehicles. Therefore, the proposed method not only can significantly reduce the average delay of vehicles but also effectively save fuel consumption of vehicles.

B. Sensitivity Analysis of Parameters

In the above simulation scenarios, the optimization time interval is 10 s. The result shows that when the optimized time interval is larger, the space for scheduling optimization is larger; that is, the percentage of delay reduction is more evident under the same simulation duration. Meanwhile, in this study, the minimum safe time interval of adjacent vehicles in the conflict and in the same direction, passing through the conflict zone also play a vital role in the proposed model. Therefore, this section would perform a sensitivity analysis of these three parameters. Traffic scenario number 4 in Table III is selected as the fixed scenario to avoid the impact of traffic volume. Firstly, the optimized time interval is set as 8 to 20 s with 2 s step. The vehicle delay is selected as the evaluation index to analyze the influence of different optimized time intervals on the performance of the proposed method. The sensitivity analysis results are shown in Fig. 4.

Fig. 4 illustrates that with the increase of the rolling optimization time interval, the average delay under the proposed method generally shows a decreasing trend. The average delay of vehicles under the FIFO method fluctuates around 90 s/veh. Theoretically, the delay of the FIFO method is not affected by the optimization interval. This is because different random numbers are used in the simulation experiment with different optimization intervals, which leads to different delay

TABLE IV
COMPARISON OF VEHICLE DELAYS

Number	Number of vehicles (veh)	The FIFO-based method (s)		The proposed method (s)		Delay reduction	
		Total	Average	Total	Average	Value (s)	Percentage
1	451	292	0.65	260	0.58	-0.07	-10.82%
2	522	962	1.84	693	1.33	-0.51	-27.75%
3	609	13,841	22.72	6,358	10.40	-12.32	-54.23%
4	754	68,109	90.33	39,471	52.36	-37.97	-42.04%
5	895	158,837	177.50	91,335	102.08	-75.42	-42.49%
6	1,049	287,445	273.98	172,225	164.16	-109.82	-40.08%

TABLE V
COMPARISON OF VEHICLE FUEL CONSUMPTION UNDER DIFFERENT METHODS AND TRAFFIC DEMANDS

Number	Number of vehicles (veh)	The FIFO-based method (mL)		The proposed method (mL)		Fuel consumption reduction	
		Total	Average	Total	Average	Value (mL)	Percentage
1	451	6,921	14.59	6,387	13.47	-1.12	-7.67%
2	522	13,480	25.82	11,019	21.11	-4.71	-18.26%
3	609	26,765	41.88	20,606	32.12	-9.76	-23.30%
4	754	69,960	74.83	49,768	53.24	-21.59	-28.85%
5	895	133,846	145.67	88,232	96.04	-49.63	-34.07%
6	1,049	225,074	184.99	147,744	121.44	-63.56	-34.36%

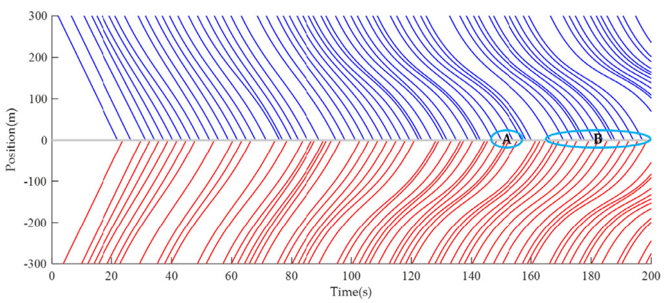

a) FIFO-based method

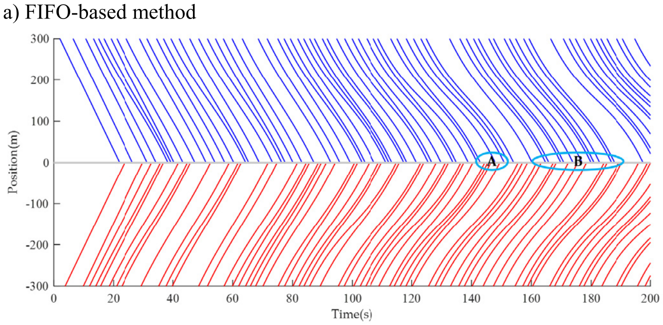

b) The proposed method

Fig. 3. Space-time trajectory (Experiment No. 3).

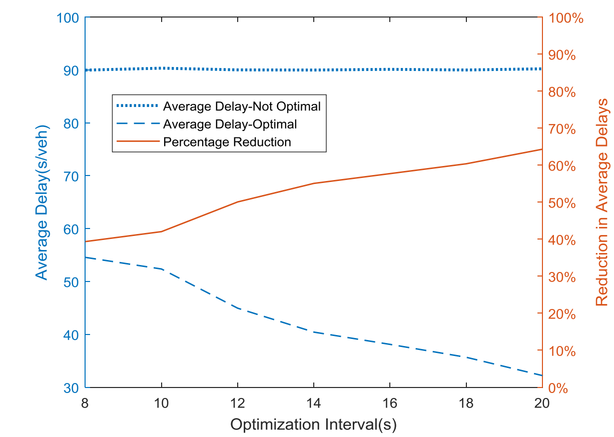

Fig. 4. Sensitivity analysis of rolling optimization time interval.

fluctuations in different optimization intervals. At the same time, compared with the FIFO-based method, the percentage reduction of the average delay under the proposed method increases with the increase of the rolling optimization time interval. Therefore, this is consistent with theoretical analysis, the larger the rolling optimization time interval, the larger the optimization space is. However, the actual rolling optimization time interval should be selected according to the length of the predicted time interval. With the large-scale application of CAVs, the time interval of vehicle arrival prediction would continue to increase [42].

Secondly, the minimum safe time interval on the performance of the proposed method is analyzed. Moreover, the minimum safe time interval of the conflict direction is 1 to 2 s, and the minimum safe time interval in the same direction is 0.5 to 1.5 s. The analysis results are shown in **Fig. 5**.

Fig. 5a) shows that as the minimum safety interval of vehicles decreases, the vehicle delay would also decrease. According to the analysis, the minimum safety interval of vehicles limits the time difference between the front and rear vehicles passing through the conflicts zone, which leads to vehicle delay. Therefore, the smaller the minimum safety interval is, the smaller vehicle delays would be. If the minimum safety time interval is zero, the vehicle will pass through the conflict zone without delay. Moreover, the dark blue region on both sides of the black straight line in **Fig. 5**b) shows that when the values of τ and ω are close, the average delay reduction percentage is smaller than the FIFO-based method. Especially, when τ is equal to ω, the percentage of delay reduction is zero. This result illustrates that when τ is equal to ω, the average delay of the vehicle is equal in both the proposed method and FIFO-based method. From the above analysis, we could know that when $\tau < \omega$, the basic principle of the proposed method is to avoid the occurrence of ω and increase the occurrence

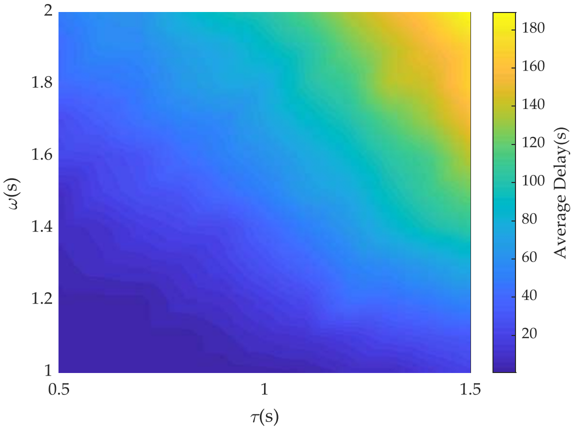

a) Average delay

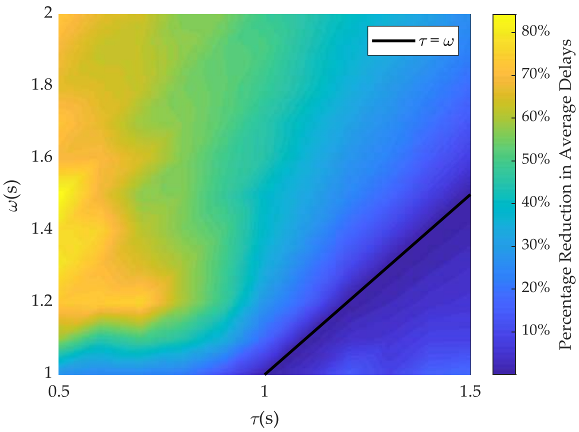

b) Average delay reduction percentage

Fig. 5. Sensitivity analysis of vehicle minimum safety interval.

of τ. Thus, the vehicle delay will be reduced by the proposed method. Nevertheless, if $\tau = \omega$, the proposed method cannot find the gap of τ and ω. In this case, the results of the proposed method are consistent with the FIFO-based method; that is, the average delay reduction percentage is zero.

The yellow area in **Fig. 5**b) shows that when the values of τ and ω differ greatly, the percentage of vehicle average delay reduction under the proposed method is more significant than that of the FIFO-based method. Therefore, this is also consistent with the above analysis. The proposed method can optimize the scheduling of vehicles and avoid the occurrence of ω and increase the occurrence of τ, thereby achieving the purpose of reducing vehicle delay. Besides, the value of ω depends on the type and size of the conflict zone, while τ is the gap for car-following. Therefore, in practical application, the reasonable value of ω should be designed according to the type and size of the conflict zone. In addition, the design of smaller safe following gap τ is conducive to reduce vehicle delay.

Pseudocode of the Simulation Experiment

Initialize:

Total simulation time T, time planning horizon ΔT, current time $t = 0, L, V_i, \tau, \omega, \theta, v_{ij}^0, v_{ij}^f, v_{\min}, v_{\max}, a_{\min}, a_{\max}, s_0, \delta$ in arm $i, \forall i \in \mathcal{I}$.

Generate the arrival times of CAVs at arm $i, \forall i \in \mathcal{I}$.

Iterate:

While $t + \Delta T \leq T$ **do**

Get the arrival times ($t_{ij}^-, \forall i \in \mathcal{I}, j \in \mathcal{N}_i$) of CAVs in time planning horizon $[t, t + \Delta T]$.

Calculate $t_{ij}^+, \forall i \in \mathcal{I}, j \in \mathcal{N}_i$ based on Eq.(1).

Optimize the scheduling of CAVs entering the conflict zone based on Eq.(12).

Obtain d

Obtain the scheduling of CAVs.

For $i = 1 \rightarrow 2$ **do**

Obtain $\mathcal{N}_i, t_{ij}^-, t_{ij}^+, \forall i \in \mathcal{I}, j \in \mathcal{N}_i$.

Optimize the CAV trajectory based on Eqs.(24-33).

Obtain $\mathcal{G}_i$.

End

Calculate g.

Save vehicle trajectories, the scheduling of CAVs, average vehicle's delay, and gasoline consumption at the current time planning horizon $[t, t + \Delta T]$.

$t \longleftarrow t + \Delta T$

End

Output:

Output vehicle trajectories, the scheduling of CAVs, average vehicle delay, and gasoline consumption at total simulation time.

VI. Conclusion and Future Work

This study proposes a two-level model to optimize scheduling and trajectories for CAVs in a conflict zone, in which the first level is a MILP to optimize the timing of vehicles entering the conflict zone, and the second level is a multi-vehicle nonlinear optimal control model to optimize vehicle trajectories. Considering the actual application requirements and complexity of the proposed method, we introduce a rolling optimization strategy. Results from a simulation experiment indicate that:

(1) Compared with the FIFO-based method, the proposed method reduces the vehicle delay and fuel consumption by optimizing the schedule of vehicles in the collision direction through the conflict zone. Through simulation results of different traffic scenarios, the vehicle delay can be reduced by up to 54.23% and the fuel consumption by up to 34.36%.

(2) The rolling optimization time interval has a significant influence on the performance of the proposed method. Moreover, the percentage reduction of the average delay increases with the increase of the rolling optimization time interval compared with the FIFO-based method.

(3) As the minimum safety interval of the vehicle decreases, vehicle delays would also decrease. When the minimum time interval $\tau = \omega$, the proposed method cannot find the gap of τ and ω to reduce vehicle delay.

(4) τ is a very important parameter of the conflict zones. The reasonable value of τ should be designed according to the type and size of the conflict zone.

This paper reveals the mechanism of improving the traffic efficiency of the conflict zones by CAVs, and puts forward a rolling optimization framework suitable for practical application. However, this work still has some limitations:

(1) Only one conflict zone, a one-way unsignalized intersection, is discussed in case study. The setting and selection of parameters for the other two conflict zones need to be further discussed in combination with the actual cases.

(2) In this study, we did not consider the possibility that vehicles cannot enter the approach because of queues. If the traffic demand is very big, the queue length over the border of the conflict zone. In this case, the demand is greater than capacity. To avoid this situation, the smaller time gap between two vehicles will be designed to improve the capacity of conflict zone.

(3) The conflict zone is too simple and contains only two conflict directions. Therefore, future work would include further investigation of scheduling and trajectory collaborative optimization methods for more complex conflict zones (such as multi-turn intersections), and traffic signals and trajectory optimization methods for mixed traffic flow of CAVs and HDVs.

Appendix

See Pseudocode of the Simulation Experiment.

References

[1] L. Zheng and T. Sayed, "Comparison of traffic conflict indicators for crash estimation using peak over threshold approach," *Transp. Res. Rec., J. Transp. Res. Board*, vol. 2673, no. 5, pp. 493–502, May 2019, doi: 10.1177/0361198119841556.

[2] S. Soleimaniamiri and X. Li, "Scheduling of heterogeneous connected automated vehicles at a general conflict area," presented at the Transp. Res. Board 98th Annu. MeetingTransportation Res. Board, Jan. 2019, Accessed: Jan. 17, 2020. [Online]. Available: https://trid.trb.org/view/1573076.

[3] T. Sayed and S. Zein, "Traffic conflict standards for intersections," *Transp. Planning Technol.*, vol. 22, no. 4, pp. 309–323, Aug. 1999, doi: 10.1080/03081069908717634.

[4] P. Włodarek and P. Olszewski, "Traffic safety on cycle track crossings–traffic conflict technique," *J. Transp. Saf. Secur.*, vol. 12, no. 1, pp. 194–209, Jun. 2019, doi: 10.1080/19439962.2019.1622615.

[5] W. Zhao, R. Liu, and D. Ngoduy, "A bilevel programming model for autonomous intersection control and trajectory planning," *Transportmetrica A, Transp. Sci.*, pp. 1–26, Jan. 2019. [Online]. Available: https://www.tandfonline.com/doi/full/10.1080/23249935.2018.1563921, doi: 10.1080/23249935.2018.1563921.

[6] Z. Yao, Y. Jiang, B. Zhao, X. Luo, and B. Peng, "A dynamic optimization method for adaptive signal control in a connected vehicle environment," *J. Intell. Transp. Syst.*, vol. 24, no. 2, pp. 184–200, Aug. 2019, doi: 10.1080/15472450.2019.1643723.

[7] Z. Yao, L. Shen, R. Liu, Y. Jiang, and X. Yang, "A dynamic predictive traffic signal control framework in a cross-sectional vehicle infrastructure integration environment," *IEEE Trans. Intell. Transp. Syst.*, vol. 21, no. 4, pp. 1455–1466, Apr. 2020, doi: 10.1109/TITS.2019.2909390.

[8] C. Yu, Y. Feng, H. X. Liu, W. Ma, and X. Yang, "Integrated optimization of traffic signals and vehicle trajectories at isolated urban intersections," *Transp. Res. B, Methodol.*, vol. 112, pp. 89–112, Jun. 2018, doi: 10.1016/j.trb.2018.04.007.

[9] Y. Guo, J. Ma, C. Xiong, X. Li, F. Zhou, and W. Hao, "Joint optimization of vehicle trajectories and intersection controllers with connected automated vehicles: Combined dynamic programming and shooting heuristic approach," *Transp. Res. C, Emerg. Technol.*, vol. 98, pp. 54–72, Jan. 2019, doi: 10.1016/j.trc.2018.11.010.

[10] Y. Feng, K. L. Head, S. Khoshmagham, and M. Zamanipour, "A real-time adaptive signal control in a connected vehicle environment," *Transp. Res. C, Emerg. Technol.*, vol. 55, pp. 460–473, Jun. 2015.

[11] H. Xu, S. Feng, Y. Zhang, and L. Li, "A grouping-based cooperative driving strategy for CAVs merging problems," *IEEE Trans. Veh. Technol.*, vol. 68, no. 6, pp. 6125–6136, Jun. 2019, doi: 10.1109/TVT.2019.2910987.

[12] C. Y. D. Yang, K. Ozbay, and X. (Jeff) Ban, "Developments in connected and automated vehicles," *J. Intell. Transp. Syst.*, vol. 21, no. 4, pp. 251–254, Jul. 2017, doi: 10.1080/15472450.2017.1337974.

[13] S. E. Shladover, "Connected and automated vehicle systems: Introduction and overview," *J. Intell. Transp. Syst.*, vol. 22, no. 3, pp. 190–200, May 2018, doi: 10.1080/15472450.2017.1336053.

[14] Z. Yao, T. Xu, Y. Jiang, and R. Hu, "Linear stability analysis of heterogeneous traffic flow considering degradations of connected automated vehicles and reaction time," *Phys. A, Stat. Mech. Appl.*, vol. 561, Jan. 2021, Art. no. 125218, doi: 10.1016/j.physa.2020.125218.

[15] P. Bansal and K. M. Kockelman, "Forecasting Americans' long-term adoption of connected and autonomous vehicle technologies," *Transp. Res. A: Policy Pract.*, vol. 95, pp. 49–63, Jan. 2017, doi: 10.1016/j.tra.2016.10.013.

[16] S. Karbalaieali, O. A. Osman, and S. Ishak, "A dynamic adaptive algorithm for merging into platoons in connected automated environments," *IEEE Trans. Intell. Transp. Syst.*, early access, Sep. 20, 2019, doi: 10.1109/TITS.2019.2938728.

[17] S. A. Fayazi and A. Vahidi, "Mixed-integer linear programming for optimal scheduling of autonomous vehicle intersection crossing," *IEEE Trans. Intell. Vehicles*, vol. 3, no. 3, pp. 287–299, Sep. 2018, doi: 10.1109/TIV.2018.2843163.

[18] Z. He, L. Zheng, L. Lu, and W. Guan, "Erasing lane changes from roads: A design of future road intersections," *IEEE Trans. Intell. Vehicles*, vol. 3, no. 2, pp. 173–184, Jun. 2018, doi: 10.1109/TIV.2018.2804164.

[19] W. Li and X. Ban, "Connected vehicles based traffic signal timing optimization," *IEEE Trans. Intell. Transp. Syst.*, vol. 20, no. 12, pp. 4354–4366, Dec. 2019, doi: 10.1109/TITS.2018.2883572.

[20] Z. Wang, G. Wu, and M. J. Barth, "Cooperative eco-driving at signalized intersections in a partially connected and automated vehicle environment," *IEEE Trans. Intell. Transp. Syst.*, vol. 21, no. 5, pp. 2029–2038, May 2020, doi: 10.1109/TITS.2019.2911607.

[21] B. Xu *et al.*, "Cooperative method of traffic signal optimization and speed control of connected vehicles at isolated intersections," *IEEE Trans. Intell. Transp. Syst.*, vol. 20, no. 4, pp. 1390–1403, Apr. 2019, doi: 10.1109/TITS.2018.2849029.

[22] Z. Yao, R. Hu, Y. Wang, Y. Jiang, B. Ran, and Y. Chen, "Stability analysis and the fundamental diagram for mixed connected automated and human-driven vehicles," *Phys. A, Stat. Mech. Appl.*, vol. 533, Nov. 2019, Art. no. 121931, doi: 10.1016/j.physa.2019.121931.

[23] S. Bang and S. Ahn, "Mixed traffic of connected and autonomous vehicles and human-driven vehicles: Traffic evolution and control using spring-mass-damper system," *Transp. Res. Rec.*, vol. 2673, no. 7, pp. 504–515, May 2019, doi: 10.1177/0361198119847618.

[24] Y. Qin and H. Wang, "Cell transmission model for mixed traffic flow with connected and autonomous vehicles," *J. Transp. Eng., A, Syst.*, vol. 145, no. 5, May 2019, Art. no. 04019014, doi: 10.1061/JTEPBS.0000238.

[25] X. He, H. X. Liu, and X. Liu, "Optimal vehicle speed trajectory on a signalized arterial with consideration of queue," *Transp. Res. C, Emerg. Technol.*, vol. 61, pp. 106–120, Dec. 2015, doi: 10.1016/j.trc.2015.11.001.

[26] L. Li and X. Li, "Parsimonious trajectory design of connected automated traffic," *Transp. Res. B, Methodol.*, vol. 119, pp. 1–21, Jan. 2019, doi: 10.1016/j.trb.2018.11.006.

[27] J. Ma, X. Li, F. Zhou, J. Hu, and B. B. Park, "Parsimonious shooting heuristic for trajectory design of connected automated traffic part II: Computational issues and optimization," *Transp. Res. B, Methodol.*, vol. 95, pp. 421–441, Jan. 2017, doi: 10.1016/j.trb.2016.06.010.

[28] X. Hu and J. Sun, "Trajectory optimization of connected and autonomous vehicles at a multilane freeway merging area," *Transp. Res. C, Emerg. Technol.*, vol. 101, pp. 111–125, Apr. 2019, doi: 10.1016/j.trc.2019.02.016.

[29] Q. Guo, L. Li, and X. (Jeff) Ban, "Urban traffic signal control with connected and automated vehicles: A survey," *Transp. Res. C, Emerg. Technol.*, vol. 101, pp. 313–334, Apr. 2019, doi: 10.1016/j.trc.2019.01.026.

[30] Y. Han and S. Ahn, "Stochastic modeling of breakdown at freeway merge bottleneck and traffic control method using connected automated vehicle," *Transp. Res. B, Methodol.*, vol. 107, pp. 146–166, Jan. 2018, doi: 10.1016/j.trb.2017.11.007.

[31] N. Wan, A. Vahidi, and A. Luckow, "Optimal speed advisory for connected vehicles in arterial roads and the impact on mixed traffic," *Transp. Res. C, Emerg. Technol.*, vol. 69, pp. 548–563, Aug. 2016, doi: 10.1016/j.trc.2016.01.011.

[32] W. Zhao, D. Ngoduy, S. Shepherd, R. Liu, and M. Papageorgiou, "A platoon based cooperative eco-driving model for mixed automated and human-driven vehicles at a signalised intersection," *Transp. Res. C, Emerg. Technol.*, vol. 95, pp. 802–821, Oct. 2018, doi: 10.1016/j.trc.2018.05.025.

[33] Y. Feng, C. Yu, and H. X. Liu, "Spatiotemporal intersection control in a connected and automated vehicle environment," *Transp. Res. C, Emerg. Technol.*, vol. 89, pp. 364–383, Apr. 2018, doi: 10.1016/j.trc.2018.02.001.

[34] L. Chen and C. Englund, "Cooperative intersection management: A survey," *IEEE Trans. Intell. Transp. Syst.*, vol. 17, no. 2, pp. 570–586, Feb. 2016, doi: 10.1109/TITS.2015.2471812.

[35] R. Tachet *et al.*, "Revisiting street intersections using slot-based systems," *PLoS ONE*, vol. 11, no. 3, Mar. 2016, Art. no. e0149607, doi: 10.1371/journal.pone.0149607.

[36] L. Li and F.-Y. Wang, "Cooperative driving at blind crossings using intervehicle communication," *IEEE Trans. Veh. Technol.*, vol. 55, no. 6, pp. 1712–1724, Nov. 2006, doi: 10.1109/TVT.2006.878730.

[37] Y. Meng, L. Li, F.-Y. Wang, K. Li, and Z. Li, "Analysis of cooperative driving strategies for nonsignalized intersections," *IEEE Trans. Veh. Technol.*, vol. 67, no. 4, pp. 2900–2911, Apr. 2018, doi: 10.1109/TVT.2017.2780269.

[38] S. A. Fayazi, A. Vahidi, and A. Luckow, "Optimal scheduling of autonomous vehicle arrivals at intelligent intersections via MILP," in *Proc. Amer. Control Conf. (ACC)*, Seattle, WA, USA, May 2017, pp. 4920–4925, doi: 10.23919/ACC.2017.7963717.

[39] K. Dresner and P. Stone, "A multiagent approach to autonomous intersection management," *J. Artif. Intell. Res.*, vol. 31, pp. 591–656, Mar. 2008, doi: 10.1613/jair.2502.

[40] J. Rios-Torres and A. A. Malikopoulos, "Automated and cooperative vehicle merging at highway on-ramps," *IEEE Trans. Intell. Transp. Syst.*, vol. 18, no. 4, pp. 780–789, Apr. 2017, doi: 10.1109/TITS.2016.2587582.

[41] Z. Wang, G. Wu, and M. Barth, "Distributed consensus-based cooperative highway on-ramp merging using V2X communications," in *Proc. SAE Tech. Paper Ser.*, Apr. 2018, pp. 01–2018, doi: 10.4271/2018-01-1177.

[42] X. Li, A. Ghiasi, Z. Xu, and X. Qu, "A piecewise trajectory optimization model for connected automated vehicles: Exact optimization algorithm and queue propagation analysis," *Transp. Res. B, Methodol.*, vol. 118, pp. 429–456, Dec. 2018, doi: 10.1016/j.trb.2018.11.002.

[43] J. B. Kenney, "Dedicated short-range communications (DSRC) standards in the united states," *Proc. IEEE*, vol. 99, no. 7, pp. 1162–1182, Jul. 2011, doi: 10.1109/JPROC.2011.2132790.

[44] J. Zhu and S. Roy, "Mac for dedicated short range communications in intelligent transport system," *IEEE Commun. Mag.*, vol. 41, no. 12, pp. 60–67, Dec. 2003, doi: 10.1109/MCOM.2003.1252800.

[45] H. Jiang, J. Hu, S. An, M. Wang, and B. B. Park, "Eco approaching at an isolated signalized intersection under partially connected and automated vehicles environment," *Transp. Res. C, Emerg. Technol.*, vol. 79, pp. 290–307, Jun. 2017, doi: 10.1016/j.trc.2017.04.001.

[46] J. N. Hooker, "Optimal driving for single-vehicle fuel economy," *Transp. Res. A, Gen.*, vol. 22, no. 3, pp. 183–201, May 1988, doi: 10.1016/0191-2607(88)90036-2.

[47] R. Akcelik, "Efficiency and drag in the power-based model of fuel consumption," *Transp. Res. B, Methodol.*, vol. 23, no. 5, pp. 376–385, Oct. 1989, doi: 10.1016/0191-2615(89)90014-3.

[48] K. Post, J. H. Kent, J. Tomlin, and N. Carruthers, "Fuel consumption and emission modelling by power demand and a comparison with other models," *Transp. Res. A, Gen.*, vol. 18, no. 3, pp. 191–213, May 1984, doi: 10.1016/0191-2607(84)90126-2.

[49] K. Ahn, "Microscopic fuel consumption and emission modeling," M.S. thesis, Dept. Civil Environ. Eng., Virginia Tech., Blacksburg, VA, USA, 1998.

[50] P. Typaldos, I. Papamichail, and M. Papageorgiou, "Minimization of fuel consumption for vehicle trajectories," *IEEE Trans. Intell. Transp. Syst.*, vol. 21, no. 4, pp. 1716–1727, Apr. 2020, doi: 10.1109/TITS.2020.2972770.

[51] G. Lu, Y. Nie, X. Liu, and D. Li, "Trajectory-based traffic management inside an autonomous vehicle zone," *Transp. Res. B, Methodol.*, vol. 120, pp. 76–98, Feb. 2019, doi: 10.1016/j.trb.2018.12.012.

Zhihong Yao received the B.S. and Ph.D. degrees in transportation engineering from Southwest Jiaotong University, Chengdu, China, in 2014 and 2019, respectively.

He also spent one year as a joint Doctoral Student at the University of Wisconsin–Madison, Madison, WI, USA. He is an Assistant Professor with the School of Transportation and Logistics, Southwest Jiaotong University. He has coauthored more than 40 articles that have been published in the IEEE TRANSACTIONS ON INTELLIGENT TRANSPORTATION SYSTEMS, the *Journal of Intelligent Transportation Systems*, *IET Intelligent Transport Systems*, *Physica A: Statistical Mechanics and Its Applications*, the *Journal of Advanced Transportation*, and *Transportation Research Record*. His research interests include traffic signal control and connected automated vehicles.

Haoran Jiang received the B.S. degree in transportation engineering from Southwest Jiaotong University, Chengdu, China, where he is currently pursuing the Ph.D. degree with the School of Transportation and Logistics. His research interests include intelligent transportation systems and connected automated vehicles.

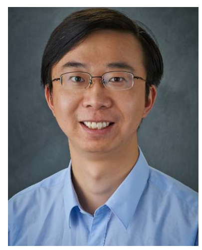

Yang Cheng (Member, IEEE) received the B.S. degree in automation and the M.S. degree in intelligent transportation systems from Tsinghua University, Beijing, China, in 2004 and 2006, respectively, and the Ph.D. degree in transportation engineering from the University of Wisconsin–Madison, Madison, WI, USA, in 2010.

From 2010 to 2011, he was a Teaching Assistant with the University of Wisconsin–Madison. From 2011 to 2013, he was a Research Associate with the Traffic Operations and Safety Laboratory, University of Wisconsin–Madison, where he has been an Assistant Researcher with the Traffic Operations and Safety Laboratory since 2013. His research interests include traffic modeling, traffic information, and intelligent transportation systems.

Yangsheng Jiang received the B.S. degree in mechanical engineering from Yanshan University, Qinhuangdao, China, in 1998, and the Ph.D. degree in transportation engineering from Southwest Jiaotong University, Chengdu, China, in 2004.

He has been working as an Assistant Professor, an Associate Professor, and a Professor with the School of Transportation and Logistics, Southwest Jiaotong University, where he is currently a Professor and the Deputy Director of the National Engineering Laboratory of Integrated Transportation Big Data Application Technology. His research interests include transportation systems optimization and traffic big data.

Bin Ran received the B.S. degree in civil engineering from Tsinghua University, Beijing, China, in 1986, the M.S. degree in civil engineering from the University of Tokyo, Tokyo, Japan, in 1989, and the Ph.D. degree in civil engineering from the University of Illinois, Chicago, IL, USA, in 1993.

From 1993 to 1994, he worked as a Post-Doctoral Researcher at the University of California at Berkley. From 1994 to 1995, he served as a Lecturer at the Massachusetts Institute of Technology. Since 1995, he has been working as an Assistant Professor, an Associate Professor, and a Professor with the Department of Civil and Environmental Engineering, University of Wisconsin–Madison, Madison, WI, USA. He became a Guest Professor at Southeast University in 2009 and has been a Professor since 2010. His research has focused on five major areas such as intelligent transportation system (ITS) technology development and system evaluation, dynamic transportation network and traffic modeling, the development of mobile probe technologies for traffic state estimation and passenger flow estimation, connected automated vehicle highway (CAVH), vehicle-highway coordination, intelligent vehicles, automated highway systems, and big data applications for multimodal transportation databases.